NASA/CR—2004-213067

Elasto-Plastic Analysis of Tee Joints Using HOT-SMAC

Brett A. Bednarcyk
Ohio Aerospace Institute, Brook Park, Ohio

Phillip W. Yarrington
Collier Research Corporation, Hampton, Virginia

May 2004

The NASA STI Program Office . . . in Profile

Since its founding, NASA has been dedicated to the advancement of aeronautics and space science. The NASA Scientific and Technical Information (STI) Program Office plays a key part in helping NASA maintain this important role.

The NASA STI Program Office is operated by Langley Research Center, the Lead Center for NASA's scientific and technical information. The NASA STI Program Office provides access to the NASA STI Database, the largest collection of aeronautical and space science STI in the world. The Program Office is also NASA's institutional mechanism for disseminating the results of its research and development activities. These results are published by NASA in the NASA STI Report Series, which includes the following report types:

- TECHNICAL PUBLICATION. Reports of completed research or a major significant phase of research that present the results of NASA programs and include extensive data or theoretical analysis. Includes compilations of significant scientific and technical data and information deemed to be of continuing reference value. NASA's counterpart of peer-reviewed formal professional papers but has less stringent limitations on manuscript length and extent of graphic presentations.

- TECHNICAL MEMORANDUM. Scientific and technical findings that are preliminary or of specialized interest, e.g., quick release reports, working papers, and bibliographies that contain minimal annotation. Does not contain extensive analysis.

- CONTRACTOR REPORT. Scientific and technical findings by NASA-sponsored contractors and grantees.

- CONFERENCE PUBLICATION. Collected papers from scientific and technical conferences, symposia, seminars, or other meetings sponsored or cosponsored by NASA.

- SPECIAL PUBLICATION. Scientific, technical, or historical information from NASA programs, projects, and missions, often concerned with subjects having substantial public interest.

- TECHNICAL TRANSLATION. English-language translations of foreign scientific and technical material pertinent to NASA's mission.

Specialized services that complement the STI Program Office's diverse offerings include creating custom thesauri, building customized databases, organizing and publishing research results . . . even providing videos.

For more information about the NASA STI Program Office, see the following:

- Access the NASA STI Program Home Page at ***http://www.sti.nasa.gov***

- E-mail your question via the Internet to help@sti.nasa.gov

- Fax your question to the NASA Access Help Desk at 301–621–0134

- Telephone the NASA Access Help Desk at 301–621–0390

- Write to:
  NASA Access Help Desk
  NASA Center for AeroSpace Information
  7121 Standard Drive
  Hanover, MD 21076

NASA/CR—2004-213067

Elasto-Plastic Analysis of Tee Joints Using HOT-SMAC

Brett A. Bednarcyk
Ohio Aerospace Institute, Brook Park, Ohio

Phillip W. Yarrington
Collier Research Corporation, Hampton, Virginia

Prepared under Cooperative Agreement NCC3–650

National Aeronautics and
Space Administration

Glenn Research Center

May 2004

Acknowledgments

The authors wish to thank Marek-Jerzy Pindera, Jacob Aboudi, Steven M. Arnold, and Craig S. Collier, for helpful discussions during the course of this investigation. The financial support through NASA Glenn Research Center Grants NCC3–650 and NCC3–878 is also gratefully acknowleged.

This work was sponsored by the Low Emissions Alternative Power Project of the Vehicle Systems Program at the NASA Glenn Research Center.

Available from

NASA Center for Aerospace Information
7121 Standard Drive
Hanover, MD 21076

National Technical Information Service
5285 Port Royal Road
Springfield, VA 22100

Available electronically at http://gltrs.grc.nasa.gov

ELASTO-PLASTIC ANALYSIS OF TEE JOINTS USING HOT-SMAC

Brett A. Bednarcyk
Ohio Aerospace Institute
Brook Park, Ohio 44142

Phillip W. Yarrington
Collier Research Corporation
Hampton, Virginia 23669

Abstract

The Higher Order Theory – Structural/Micro Analysis Code (HOT-SMAC) software package is applied to analyze the linearly elastic and elasto-plastic response of adhesively bonded tee joints. Joints of this type are finding an increasing number of applications with the increased use of composite materials within advanced aerospace vehicles, and improved tools for the design and analysis of these joints are needed. The linearly elastic results of the code are validated vs. finite element analysis results from the literature under different loading and boundary conditions, and new results are generated to investigate the inelastic behavior of the tee joint. The comparison with the finite element results indicates that HOT-SMAC is an efficient and accurate alternative to the finite element method and has a great deal of potential as an analysis tool for a wide range of bonded joints.

1. Introduction

The application of adhesive bonding within the aircraft industry is rapidly expanding. As advanced composite materials are being used more extensively on new and developing aerospace vehicles, so too are the adhesive joints that have been shown to have certain advantages over mechanically fastened joints (i.e., riveted or bolted) for these lightweight structures (Adams and Wake, 1984). While a great deal of research has investigated the analysis and design of adhesive joints, especially for the simpler joint geometries (c.f., Hart-Smith, 1973a-c; Yuceoglu and Updike, 1981; Adams and Wake, 1984; Pickett and Hollaway, 1985; Mortensen and Thomsen, 2002), the joints within a large aerospace structure are often treated as an afterthought rather than an active participant in the structural system design. The reason for this trend is that the joint analysis is usually complex and cumbersome requiring many simplifying assumptions to derive an analytical solution (which are still often quite complex), or expensive finite element analysis (FEA) modeling in order to capture more accurate geometry and loading conditions. With the next generation of aerospace vehicles requiring extensive primary use of composites to meet their design specifications, the need for improved adhesively bonded joint design and analysis techniques is clear.

This paper seeks to advance an alternative to the finite element method for the accurate analysis of adhesively bonded joints. The Higher Order Theory – Structural/Micro Analysis Code (HOT-SMAC) software package, developed by NASA Glenn Research Center, Collier Research Corporation, the University of Virginia, and the Ohio Aerospace Institute, serves as this alternative. HOT-SMAC is a graphical package built upon the Higher Order Theory for Functionally Graded Materials (HOTFGM), which, as the name implies, was originally developed for analysis of functionally graded materials (FGMs). HOTFGM explicitly couples micro and macro mechanical effects, which can be important in FGMs and large fiber diameter composites. Like the finite element method, HOTFGM employs a discretized geometry, however, it differs from FEA in that a variation principal is not employed and there are no nodes. HOTFGM, rather, is based on a volume averaging technique that allows the theory to be far less sensitive to geometric discretization than FEA while retaining the ability to capture field concentrations by refining the geometric

representation (Pindera and Dunn, 1997). Further, the HOT-SMAC software provides a complete pre-processing, analysis code execution, and post-processing environment that enables an efficient procedure for the entire analysis cycle. Thus, its efficiency lies not only in the code's computational speed, but also in the time saved in setting up the problem and examining the results.

The focus of this paper is a comparison between HOT-SMAC and an FEA investigation from the literature on an adhesively bonded tee joint (see Fig. 1). The two loading conditions considered are a tensile pull-off load applied to the top of the vertical plate adherend and a side load, also applied at the top of the vertical plate. Clearly, this geometry and loading is considerably more complex than most "standard" joint configurations, and formulating a reasonably accurate analytical model would be a considerable challenge. However, this type of joint and others like it are being considered for use in many advanced aircraft as (for example) ribs must be bonded to composite skin face sheets. While the present comparison with FEA involves isotropic steel adherends, HOT-SMAC can currently analyze certain anisotropic laminates (with orthogonal plies), and a generalization to admit arbitrary laminates is under development. Linearly elastic stress fields from the FEA analysis and HOT-SMAC are compared and discussed, and the HOT-SMAC analyses are taken into the inelastic regime to investigate the yielding and plastic deformation in the adhesive and steel adherends.

2. HOT-SMAC Model and Software

The Higher Order Theory – Structural/Micro Analysis Code (HOT-SMAC) is a user-friendly graphics-based software package built around the well-established Higher Order Theory for Functionally Graded Materials (HOTFGM). The HOTFGM theoretical development is well-documented in the literature (Aboudi et al., 1999), as is its application to functionally graded composite materials (Aboudi et al., 1997), thermal barrier coatings (Pindera et al., 1998, 2002), actively cooled components (Arnold et al., 2001), and interface effects (Pindera et al., 1999).

The geometry considered by the two-dimensional version of HOTFGM (which has been implemented within HOT-SMAC) is shown in Fig. 2. The material is divided into an arbitrary number of rectangular cells, each consisting of two subcells in each in-plane direction. A cell may also contain a void rather than a material, which enables the model to admit arbitrary cross-sectional geometries, provided they can be constructed of rectangular cells (see Arnold et al., 2001). Thermal and mechanical boundary conditions are applied at all material boundaries (including those between material subcells and voids), and the thermal and mechanical structural/micromechanics problem is solved.

The HOTFGM thermal problem employs a second order temperature field expansion within each subcell ($\beta\gamma$) of the form,

$$T^{(\beta\gamma)} = T^{(\beta\gamma)}_{(00)} + \bar{x}_2^{(\beta)} T^{(\beta\gamma)}_{(10)} + \bar{x}_3^{(\gamma)} T^{(\beta\gamma)}_{(01)} + \frac{1}{2}\left(3\bar{x}_2^{(\beta)2} - \frac{1}{4} h_\beta^{(q)2} \right) T^{(\beta\gamma)}_{(20)} + \frac{1}{2}\left(3\bar{x}_3^{(\gamma)2} - \frac{1}{4} l_\gamma^{(r)2} \right) T^{(\beta\gamma)}_{(02)} \qquad (1)$$

where $\bar{x}_2^{(\beta)}$ and $\bar{x}_3^{(\gamma)}$ are the local coordinates for subcell $\beta\gamma$ (see Fig. 2), $h_\beta^{(q)}$ and $l_\gamma^{(r)}$ are height and length of the subcell, and $T^{(\beta\gamma)}_{(mn)}$ are unknown coefficients whose solution determines the temperature field. The formulation (Aboudi et al., 1999) involves satisfaction of the heat equation, as well as its first and second moments in a volumetric sense within each subcell. The thermal continuity conditions and the appropriate thermal boundary conditions are also imposed in an average sense along the applicable subcell interfaces and edges to arrive at a system of $20\, N_q\, N_r$ linear algebraic equations,

$$\boldsymbol{\kappa}\,\mathbf{T} = \mathbf{t} \qquad (2)$$

where N_q and N_r are the number of cells in the x_2- and x_3-directions, which, when solved provides the unknown temperature field coefficients, $T_{(mn)}^{(\beta\gamma)}$, present in eq. (1) and contained in the vector **T**.

The HOTFGM mechanical formulation involves a second order displacement field of the form,

$$u_1^{(\beta\gamma)} = x_1 \bar{\varepsilon}_{11} \tag{3}$$

$$u_2^{(\beta\gamma)} = W_{2(00)}^{(\beta\gamma)} + \bar{x}_2^{(\beta)} W_{2(10)}^{(\beta\gamma)} + \bar{x}_3^{(\gamma)} W_{2(01)}^{(\beta\gamma)} + \frac{1}{2}\left(3\bar{x}_2^{(\beta)2} + \frac{1}{4} h_{\beta}^{(q)2}\right) W_{2(20)}^{(\beta\gamma)} + \frac{1}{2}\left(3\bar{x}_3^{(\gamma)2} + \frac{1}{4} l_{\gamma}^{(r)2}\right) W_{2(02)}^{(\beta\gamma)} \tag{4}$$

$$u_3^{(\beta\gamma)} = W_{3(00)}^{(\beta\gamma)} + \bar{x}_2^{(\beta)} W_{3(10)}^{(\beta\gamma)} + \bar{x}_3^{(\gamma)} W_{3(01)}^{(\beta\gamma)} + \frac{1}{2}\left(3\bar{x}_2^{(\beta)2} + \frac{1}{4} h_{\beta}^{(q)2}\right) W_{3(20)}^{(\beta\gamma)} + \frac{1}{2}\left(3\bar{x}_3^{(\gamma)2} + \frac{1}{4} l_{\gamma}^{(r)2}\right) W_{3(02)}^{(\beta\gamma)} \tag{5}$$

where $W_{i(mn)}^{(\beta\gamma)}$ now serve as unknown coefficients and plain strain or generalized plane strain may be applied in the x_1-direction. The equations of equilibrium, as well as the first and second moments of these equations, are satisfied in a volumetric sense within each subcell, and mechanical continuity and boundary conditions are imposed in an average sense to arrive at a system of $40\, N_q\, N_r$ linear algebraic equations,

$$\mathbf{KU} = \mathbf{f} + \mathbf{g} \tag{6}$$

where the vector **U** contains the unknown coefficients, $W_{i(mn)}^{(\beta\gamma)}$, the vector **f** contains information of on the mechanical boundary conditions and thermal loading effects, and the vector **g** contains inelastic terms. Recently, Bansal et al. (2003) have developed a reformulated version of the HOTFGM equations that eliminates the need for the generic cell and improves the efficiency of the model by reducing the number of equations represented in eqs. (2) and (6).

The HOT-SMAC software provides a graphical environment for pre-processing, executing thermo-elasto-plastic HOTFGM simulations, and post-processing the results. A detailed description of the software is provided by Yarrington (2001). Figure 3 provides a sample screen shot of the HOT-SMAC software interface. As Fig. 3 shows, the interface is divided into seven tabs, each defining a specific aspect of a given problem. The "Setup" tab allows the general problem attributes to be specified and the constituent material properties to be input or imported. The "Geometry" tab is used to specify the cross-sectional geometry (i.e., the number and dimensions of the subcells contained in the subcell grid). HOT-SMAC can automatically grade the subcell dimensions in one or both in-plane directions. The "Materials" tab allows the constituent materials to be placed within individual, or ranges of, subcells. This too is the tab employed to replace cells with voids or "windows". Tools located on the "Materials" tab also enable the automatic functional grading of the microstructure between two materials over any range of subcells. The "Thermal B.C." and "Mechanical B.C." tabs allow application of the boundary conditions, and the "Analysis Options" tab is used to specify information on the applied loading history and the desired output data. The "Analyze" button (located at the upper right, see Fig. 3) executes the HOT-SMAC problem, and the results are automatically displayed on the "Results" tab. Here, time-dependent line plots, x-y plots, and color coded fringe plots (of the type presented herein) can be displayed. In sum, the HOT-SMAC software provides an efficient and user-friendly environment for the entire analysis cycle of HOTFGM problems.

3. Results and Discussion

HOT-SMAC analyses were performed on the tee joint configurations considered by Apalak et al. (1996). These authors analyzed the tee joint with double support shown in Fig. 1 using the MSC/NASTRAN finite element package. In addition to the dimensions indicated in Fig. 1 and Table 1, Apalak et al. (1996)

considered support lengths (a) of 10 mm and 20 mm, which are not considered herein. Further, Apalak et al. (1996) explicitly included the adhesive spew fillet in their analyses. This fillet is neglected in the present HOT-SMAC analyses for simplicity. It could be included by approximating the angled fillet surface with a discrete stepped pattern, but an actual angled boundary cannot presently be modeled by HOT-SMAC due to the rectangular shape of the subcells. The plates as well as the supports were modeled as steel with the elastic properties given in Table 2. Table 2 also provides the elastic properties for the adhesive material employed by Apalak et al. (1996). The analyses performed herein, unlike the work of Apalak et al. (1996), also consider the inelastic response of the adhesive and the steel using an incremental bilinear plasticity constitutive model (Mendelson, 1968). The additional material parameters employed to model the steel and adhesive plastic behavior (yield stress and post-yield secondary or "hardening" slope) are also given in Table 2.

Apalak et al. (1996) modeled the response of the tee joint to tensile and compressive loading (P_1) applied to the top face of the vertical plate, as well as a side load (P_3) applied at the top of the vertical plate. The present investigation considers only the tensile top face load (P_1), in addition to the side load (P_3), as shown in Fig. 4. Because the loading does not vary along the joint (in the depth-direction), the tee joint problem was treated as plane strain. Two sets of boundary conditions were considered by Apalak et al. (1996), which are also considered herein. The first treats the vertical plate as being bonded to a rigid, or fixed base, and does not actually model the horizontal plate (see Fig. 5a). The second set of boundary conditions (Fig. 5b) does include the bottom plate, with the horizontal plate pinned on either end at the midpoint of its thickness. The following two subsections discuss, in turn, the results for the loading conditions P_1 and P_3.

3.1 Top Face Loading (P_1)

Due to the symmetry of the top face loading problem (see Fig. 4a), only one half of the tee joint geometry was analyzed in this case using symmetric boundary conditions along the middle of the vertical plate. Regarding the magnitude of the applied load, Apalak et al. (1996) state that a top face load, P_1, of "500 N mm^{-1}" was applied and distributed "along the upper end of the vertical plate". Conventionally, this statement implies that a load per unit depth of 500 N/mm was distributed along the top face, which has a dimension of t/2 = 2.5 mm (due to the employed one half model with symmetry), see Fig. 1 and Table 1. Thus the applied tensile traction on the top face in the x_2-direction would be (500 N/mm) / 2.5 mm = 200 MPa. However, examining the results presented by Apalak et al. (1996) indicates the tensile normal stress in the vertical plate approaches 2.00 MPa as the distance from the supports increases (see Fig. 7b). Thus, it is most likely that Apalak et al. (1996) actually employed a total load of P_1 = 500 N, which was distributed over the entire one half model top face of dimensions W × ½ t such that σ_2 = (500 N) / (100 mm × 2.5 mm) = 2.00 MPa. Therefore, the load per unit depth, P_1, employed herein is 500 N / 100 mm = 5 N/mm.

Figure 6 shows the HOT-SMAC subcell grids employed for the top face loading condition with the two sets of boundary conditions. Recall that, due to the use of symmetry conditions along the right boundary in Fig. 6, only one half of the tee joint geometry is modeled (see Fig. 1). In addition, it was determined that employing the full 100 mm length of the vertical plate was not necessary. Provided the top face of the vertical plate (where the load is applied) is sufficiently far from the joint, the HOT-SMAC results are identical for much smaller vertical plate lengths. In order to reduce the number of subcells required, a vertical plate length of 40 mm was employed (see Fig. 6). Note that, in the case of the inelastic simulations, such a simplification requires that the plastic zone does not extend into the area that is neglected.

Both the horizontal and vertical plates, as well as the supports, were modeled using eight through-thickness subcells. The adhesive, though much thinner, was also modeled using eight through-thickness subcells. The fixed base boundary condition grid employed a total of 1296 subcells, while the flexible base grid employed a total of 1776 subcells. In the case of the flexible base, the pinned boundary condition (see Fig. 5b) was imposed by fixing (i.e., imposing zero average displacement) the middle two subcells of the horizontal plate along the left face.

Figures 7 and 8 compare the HOT-SMAC predicted stress fields with the FEA results of Apalak et al. (1996) for top face loading (P_1) for the two sets of boundary conditions (see Fig. 5). It should be noted

that the FEA results show only a part of the analyzed geometry, while the HOT-SMAC results show the entire geometry analyzed. In addition, for the load magnitude applied, the HOT-SMAC results indicated that no yielding takes place, and thus the problem results (as in the case of the FEA) remain completely linearly elastic. Despite the fact that the HOT-SMAC analyses did not explicitly model the adhesive spew fillet as was done in the FEA models, the agreement between HOT-SMAC and FEA is excellent. Qualitatively, the stress fields are virtually identical. Quantitatively, while the absolute minimum and maximum values quoted in the FEA results differ slightly from those evident in the HOT-SMAC results, comparing the actual contours between the two sets of results indicates excellent agreement. Further, some discrepancy in the highest concentrations predicted is expected due to the highly refined mesh employed by Apalak et al. (1996) in joint and fillet regions. Finally, the HOT-SMAC results in Fig. 8, which show the entire half model of the bottom plate, indicate stress concentrations associate with the boundary condition applied along the left face of the horizontal plate. Because Apalak et al. (1996) showed only a detail of the geometry in their results, it is unclear whether or not a similar concentration is present in the FEA results.

It is clear that HOT-SMAC does an excellent job of analyzing the tee joint problem for the applied top face (P_1) loading. In addition, HOT-SMAC is extremely efficient, not only in terms of the model execution time, but also in terms of the analysis cycle time required to set up the problem and post-process the results. The actual execution time was approximately 6.5 seconds for the fixed base problem and 6.9 seconds for the flexible base problem, where a 2.5 GHz desktop computer with 1 GB of RAM was used. However, the most beneficial aspect of the HOT-SMAC software is its graphical user interface that allows the problem to be set up, solved, the results displayed, and the problem altered and executed again in an extremely quick and easy manner.

As discussed above, the P_1 loading applied to the tee joint by Apalak et al. (1996) did not (according to the HOT-SMAC predictions) lead to any inelastic deformation in the adhesive or steel adherends. To simulate yielding in the tee joint, HOT-SMAC analyses were performed for the flexible base boundary conditions in which the applied top face load (P_1) was increased to ten times that applied previously (i.e., 50 N/mm). Recall that a bilinear plasticity model, available within HOT-SMAC, has been employed and the inelastic material parameters are given in Table 2. In presence of the employed plasticity model, the loading must be applied incrementally and the problem solved iteratively at each increment of the applied loading. In the present case, 100 increments were employed with a maximum of ten iterations permitted at each increment. Even in the presence of plasticity, the HOT-SMAC execution remains very efficient, requiring only approximately 35 seconds for the entire analysis.

The results of the HOT-SMAC analysis of the inelastic tee joint subjected to top face normal loading (P_1) are shown in Fig. 9. This figure shows the equivalent plastic strain field, ε_p,

$$\varepsilon_p = \int \sqrt{2/3\ \Delta\varepsilon_{ij}^p \Delta\varepsilon_{ij}^p} \tag{7}$$

where $\Delta\varepsilon_{ij}^p$ are the plastic strain component increments, at three points in the applied incremental loading history: P_1 = 30 N/mm, P_1 = 40 N/mm, and P_1 = 50 N/mm (which correspond to six, eight, and ten times the load applied for the previous results shown in Figs. 7 and 8). Figure 10 shows the evolution of the equivalent plastic strain in 18 individual subcells in the regions that undergo inelastic deformation. Yielding begins in the adhesive at the left face of the joint between the support and the horizontal plate at an applied load level of 27.5 N/mm (row 9, column 13 in Fig. 10). The plastic zone then grows within the adhesive as the loading is increased. At an applied load level of 37 N/mm, yielding begins in the horizontal steel plate at the left face where the boundary conditions are applied (row 4, column 1 in Fig. 10). The magnitude of the equivalent plastic strain at this location is too small to be seen in Fig. 9b, but the plastic deformation in the steel is evident in Fig. 9c. The location of the inelastic deformation in the adhesive (i.e., at the free edge) suggests that the predicted yielding and subsequent flow behavior may change considerably were a spew fillet included in the simulation. This issue should be explored in future work.

3.2 Side Loading (P_3)

In the case of side loading along the top edge of the vertical plate (see Fig. 4b), the symmetry present in the case of the top face loading is now absent. Thus, the entire (cross-sectional) geometry of the tee joint must be modeled. As in the case of top face loading (P_1), there is some question as to the actual magnitude of the side load (P_3) applied in the FEA of Apalak et al. (1996). These authors state that a side load of "500 N" was "applied to the node at the upper left corner of the vertical plate". Conventionally, one would expect this loading to be a load per unit depth in a plane strain problem such as this. One might interpret the loading to be a load per unit depth of 5 N/mm that has been summed over the 100 mm depth of the plate (see Fig. 1 and Table 1) to arrive at a total load of 500 N. However, for the reasons discussed below, it seems that Apalak et al. (1996) actually employed a side load (P_3) of 10 N/mm, possibly doubling the P_1 distributed load magnitude to account for the fact that the entire 5 mm width of the vertical plate (rather than one half) is now explicitly modeled.

Using simple beam theory results as bounds, it can be shown that that these authors' results are more consistent with a side load of 10 N/mm rather than 5 N/mm. As shown in Fig. 11, we consider the portion of the vertical plate above the tee joint supports as a cantilever beam subjected to the identical side loading (P_3). This cantilever beam problem should serve as an upper bound of the longitudinal stresses (σ_2) that result in the vertical plate of the tee joint problem because, while the cantilever beam employs a "built in" boundary condition, the vertical plate is embedded in the flexible tee joint supports. According to beam theory, the maximum longitudinal stress in the beam occurs at the base and has magnitude,

$$\sigma_2^{\max} = \frac{F_3 L t}{2I} \tag{8}$$

where $I = \frac{1}{12} W t^3$ is the moment of inertia and F_3 is the total force exerted by the distributed load P_3 (i.e., $F_3 = W P_3$). Substituting, we arrive at,

$$\sigma_2^{\max} = \frac{6L}{t^2}\left(\frac{F_3}{W}\right) = \frac{6 L P_3}{t^2} \tag{9}$$

and with L = 80 mm and t = 5 mm, $\sigma_2^{\max} = (19.2\ \text{mm}^{-1}) P_3$. If P_3 were 5 N/mm (as suggested by Apalak et al., 1996), $\sigma_2^{\max} = 96$ MPa would result in the cantilever beam and should serve as an upper bound for the longitudinal stress in the vertical plate. However, examining the FEA results of Apalak et al. (1996) (see Figs. 13b and 14b) indicates that the maximum longitudinal stress in the vertical plate of the tee joint is much higher, reaching 160 MPa and remaining as high as 124 MPa at a distance 15 mm above the supports. Were the applied load P_3 equal to 10 N/mm rather than 5 N/mm, the upper bound suggested by beam theory would be 192 MPa, which seems to be consistent with the FEA results of Apalak et al. (1996) (see Figs. 13b and 14b). It was thus assumed in the present investigation that a side load per unit depth (P_3) of 10 N/mm was actually applied in the FEA work of these previous authors. As mentioned previously, it is possible that Apalak et al. (1996) doubled the applied top face load per unit depth, P_1, of 5 N/mm, which had been applied in the one half symmetry model to account for the fact that, when considering the side load (P_3), the entire geometry must be modeled.

The HOT-SMAC subcell grids employed to model the response of the tee joint to the side load for the cases of fixed support and flexible support are shown in Fig. 12. Due to the lack of symmetry necessitating the simulation of the entire geometry, the number of subcells has doubled from the top loading case to 2592 and 3522 subcells, respectively, for the two grids. The side load was applied as an average traction in the x_3-direction on the left face of the subcell at the upper left corner of the vertical plate. Execution times for the problem also increased to 14 and 16 seconds, respectively. The HOT-SMAC predicted stress fields for the side loaded (P_3 = 10 N/mm) tee joint with fixed and flexible support are shown in Figs. 13 and 14, respectively. Note that the HOT-SMAC results in these figures, like the FEA results,

show only a portion (i.e., detail) of the overall joint geometry. As in the case of top face loading, the applied load does not result in any simulated yielding within the tee joint, rather the analysis remains completely linear elastic (as is the FEA analysis).

Once again, HOT-SMAC has done an excellent job, both qualitatively and quantitatively, of capturing the stress fields in the tee joint. The excellent agreement between the HOT-SMAC and FEA results for the longitudinal stress in the vertical plate (Figs. 13b and 14b) reinforces the assertion that the applied side load is truly 10 N/mm in both cases. The largest discrepancy between the two sets of results appears to be in the absolute maximum and minimum concentrations in the shear stress (σ_{23}) fields. The HOT-SMAC shear stress fields appear to be shifted towards the negative end of the scale compared to the FEA results. This is probably due to the fact that the FEA analyses included the spew fillet and employed a highly refined element mesh in the regions of the highest shear stress gradients (where the vertical plate first enters the supports).

As in the top face loading results, we once again wish to examine yielding within the tee joint for the flexible base configuration. Thus, the loading was again increased by ten times and applied in 100 increments with a maximum of ten iterations permitted at each applied loading increment. Figure 15 shows the equivalent plastic strain fields (see eq. (7)) predicted by HOT-SMAC at applied side load (P_3) levels of 20 N/mm, 40 N/mm, 60 N/mm, 80 N/mm, and 100 N/mm. Note that, again, only a portion of the total geometry is shown in Fig. 15. Figure 16 plots the evolution of the equivalent plastic strain in three individual subcells (two adhesive subcells and one steel subcell). Yielding begins in the adhesive at the joint between the vertical plate and the supports where the vertical plate first enters the supports at an applied load level of 15 N/mm (see row 48, column 56 in Fig. 16) . Soon there after, at an applied load of 19 N/mm, yielding begins in the vertical steel plate at the surfaces directly adjacent to the plastically deforming adhesive (see row 49, column 57 in Fig. 16). This yielding in the steel plate cannot yet be seen in Fig. 15a, but it is evident in Fig. 15b. Then, at an applied load level of 26 N/mm, yielding begins in the adhesive between the support and the horizontal plate at the right and left faces of the supports (see row 9, column 13 in Fig. 16). As the magnitude of the applied loading increases, the size of the plastic zone and the magnitude of the equivalent plastic strain increase. At an applied side load level of 100 N/mm, the plastic zone in the vertical plate has clearly grown through the entire thickness of this plate. The location of this "plastic hinge" formation corresponds to that of a high shear stress concentration evident in the elastic results (see Fig. 14c).

As was the case in the top face loading inelastic simulation, the fact that the inelastic deformation begins and tends to be concentrated near the free edges of the adhesive suggests that the predicted yielding and subsequent flow behavior would be affected by including a spew fillet in the simulation. The execution time for the inelastic simulation for side loaded tee joint with flexible support was approximately 76 seconds.

4. Conclusions

The elastic and elasto-plastic behavior of a tee joint consisting of steel adherends has been investigated using the Higher Order Theory – Structural/Micro Analysis Code (HOT-SMAC). The purpose of the study was to evaluate the accuracy and utility of HOT-SMAC for analyzing joints with non-standard geometries subjected to more complex loading conditions (compared to, for example, traditional single and double lap joints subjected to in-plane loading). To assess the accuracy of HOT-SMAC in terms of the predicted stress fields, results were compared to an extensive linearly elastic finite element investigation of the tee joint conducted by Apalak et al. (1996). The HOT-SMAC results exhibit excellent agreement with these finite element results for tee joints with both fixed and flexible base and both normal top face (i.e., pull-off) and side loading. The HOT-SMAC analyses (unlike the FEA) were also taken into the inelastic regime for both types of loading for the case of flexible base. The HOT-SMAC inelastic analyses were able to track the initiation and evolution of yielding and plastic flow in the adhesive and adherends throughout the tee joint in an extremely efficient manner.

The present study has clearly demonstrated the utility of HOT-SMAC for modeling joint configurations for which analytical solutions do not exist and would therefore usually fall within the realm of finite element analysis. While HOT-SMAC is extremely efficient in terms of execution time, even in the

inelastic regime, its greatest benefit comes from its impact on the efficiency of the entire analysis cycle. Thanks to its integrated graphical user interface, joint problems such as those analyzed herein can be configured (i.e., the materials, geometry, and boundary conditions specified), executed, and the results graphically displayed in a matter of minutes. Then, changes can be easily made to the problem configuration and the analysis cycle repeated quickly.

The results presented herein also suggest some areas for additional work with HOT-SMAC on this tee joint configuration. First, the geometry could be altered to include the adhesive spew fillet, as was done in the FEA analyses of Apalak et al. (1996). This, coupled with additional refinement of the subcell grid would enable comparison of the local stresses in the adhesive between HOT-SMAC and the FEA results. A study of the effects of grid refinement on the inelastic predictions is also warranted as a refined grid leads to higher stress concentrations, which would then lead to more plastic deformation. Determining the level of grid refinement needed to best represent reality would be the ultimate goal. Finally, generalizing the HOT-SMAC software to admit anisotropic constituent materials and three-dimensional geometries would enable the analysis of complex joints in which the adherends are laminated composite plates. This would enable the software to address many more joint problems that are important in modern aerospace structures, and the required effort is thus certainly justified.

References

Aboudi, J., Pindera, M-J., and Arnold, S.M. (1997) "Microstructural Optimization of Functionally Graded Composites Subjected to a Thermal Gradient via the Coupled Higher-Order Theory" *Composites: Part B* **28**, 93-108.

Aboudi, J., Pindera, M-J., and Arnold, S.M. (1999) "Higher-Order Theory for Functionally Graded Materials" *Composites: Part B* **30**, 777-832.

Adams, R.D. and Wake, W.C. (1984) *Structural Adhesive Joints in Engineering*, Elsevier, London.

Apalak, Z.G., Apalak, M.K, and Davies, R. (1996) "Analysis and Design of Tee Joints with Double Support" *International Journal of Adhesion and Adhesives* **16**, 187-214.

Arnold, S.M., Bednarcyk, B.A., and Aboudi, J. (2001) "Thermo-Elastic Analysis of Internally Cooled Structures Using a Higher Order Theory" NASA/TM-2001-210702.

Bansal, Y., Zhong, Y., and Pindera, M.-J. (2003) "An Efficient Reformulation of the Higher-Order Theory for FGMs" *Materials Science Forums*, **423-425**, 769-776.

Hart-Smith. L.J. (1973a) "Adhesive-Bonded Double-Lap Joints" NASA-CR-112235.

Hart-Smith. L.J. (1973b) "Adhesive-Bonded Single-Lap Joints" NASA-CR-112236.

Hart-Smith. L.J. (1973c) "Adhesive-Bonded Scarfed and Stepped-Lap Joints" NASA-CR-112237.

Mendelson, A. (1968) *Plasticity: Theory and Application*, Krieger Publishing Co., Malabar, FL.

Mortensen, F. and Thomsen, O.T. (2002) "Analysis of Adhesive Bonded Joints: A Unified Approach" *Composites Science and Technology* **62**, 1011-1031.

Pickett, A.K. and Hollaway, L. (1985) "The Analysis of Elasto-Plastic Adhesive Stress in Adhesive Bonded Lap Joints in F.R.P-Structures" *Composite Structures* **4**, 135-160.

Pindera, M.-J., Aboudi, J., and Arnold, S.M. (1998) "Thermomechanical Analysis of Functionally Graded Thermal Barrier Coatings with Different Microstructural Scales" *Journal of the American Ceramics Society*, **81**(6), 1525-1536.

Pindera, M.-J.; Aboudi, J.; and Arnold, S.M. (1999) "The Effect of Interface Roughness and Oxide Film Thickness on the Inelastic Response of Thermal Barrier Coatings to Thermal Cycling" NASA/TM-1999-209770.

Pindera, M-J., Aboudi, J., and Arnold, S. M. (2002) "Analysis of Spallation Mechanism in Thermal Barrier Coatings with Graded Bond Coats Using the Higher-Order Theory for FGMs" *International Journal of Engineering Fracture Mechanics* **69**, 1587-1606.

Pindera, M.-J. and Dunn, P. (1997) "Evaluation of the Higher-Order Theory for Functionally Graded Materials Via the Finite Element Method" *Composites: Part B* **28**, 109-119.

Yarrington, P. (2001) "User's Manual and Final Report for HOT-SMAC GUI Development" NASA/CR-2001-211294.

Yuceoglu, U. and Updike, D.P. (1981) "Bending and Shear Deformation Effects in Lap Joints" *Journal of Engineering Mechanics* **107**, 55-76.

Table 1. Tee joint dimensions.

Dimension	Symbol	Length
Plate Length	L	100 mm
Plate Width (Depth)	W	100 mm
Support Length	a	20 mm
Plate/Support Thickness	t	5 mm
Adhesive Thickness	δ	0.5 mm

Table 2. Elastic (Apalak et al., 1996) and plastic material parameters.

	Elastic Modulus (GPa)	Poisson's Ratio	Yield Stress (MPa)	Post-Yield Slope (GPa)
Steel	210	0.29	250	10.5
Adhesive	3.33	0.34	33.3	1.334

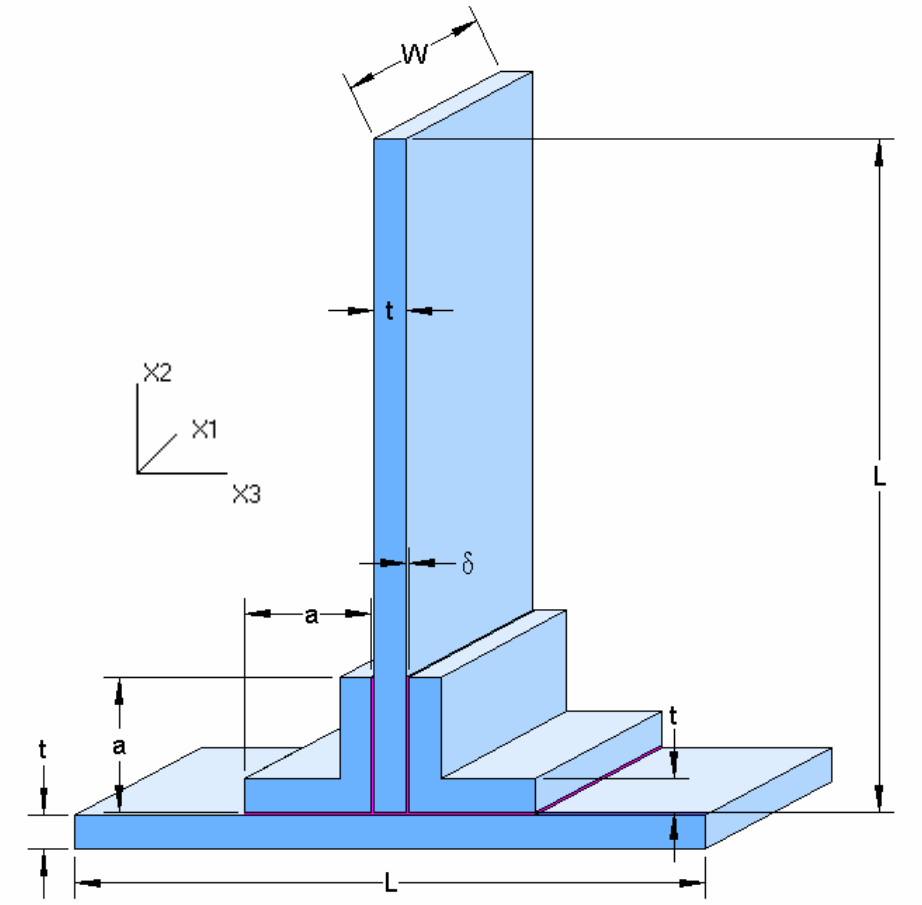

Fig. 1. Tee joint geometry and dimensions. The plates and supports shown in blue are steel, while the thin adhesive is shown in magenta.

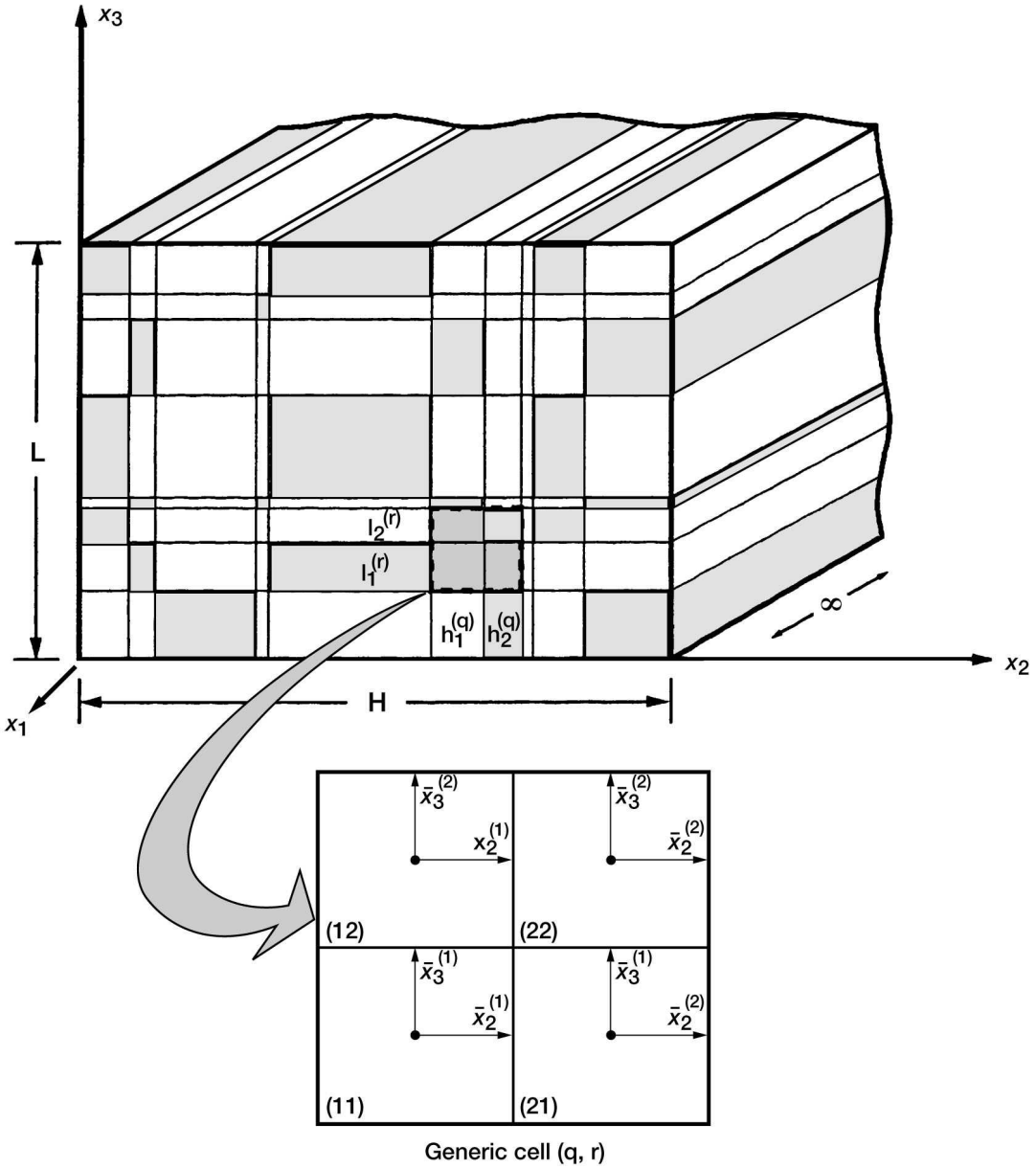

Fig. 2. HOTFGM analysis geometry. The two-dimensional geometry is discretized into cells consisting of four subcells. Cells can also be replaced by voids or "windows". Thermal and mechanical boundary conditions are applied to external, as well as window, edges.

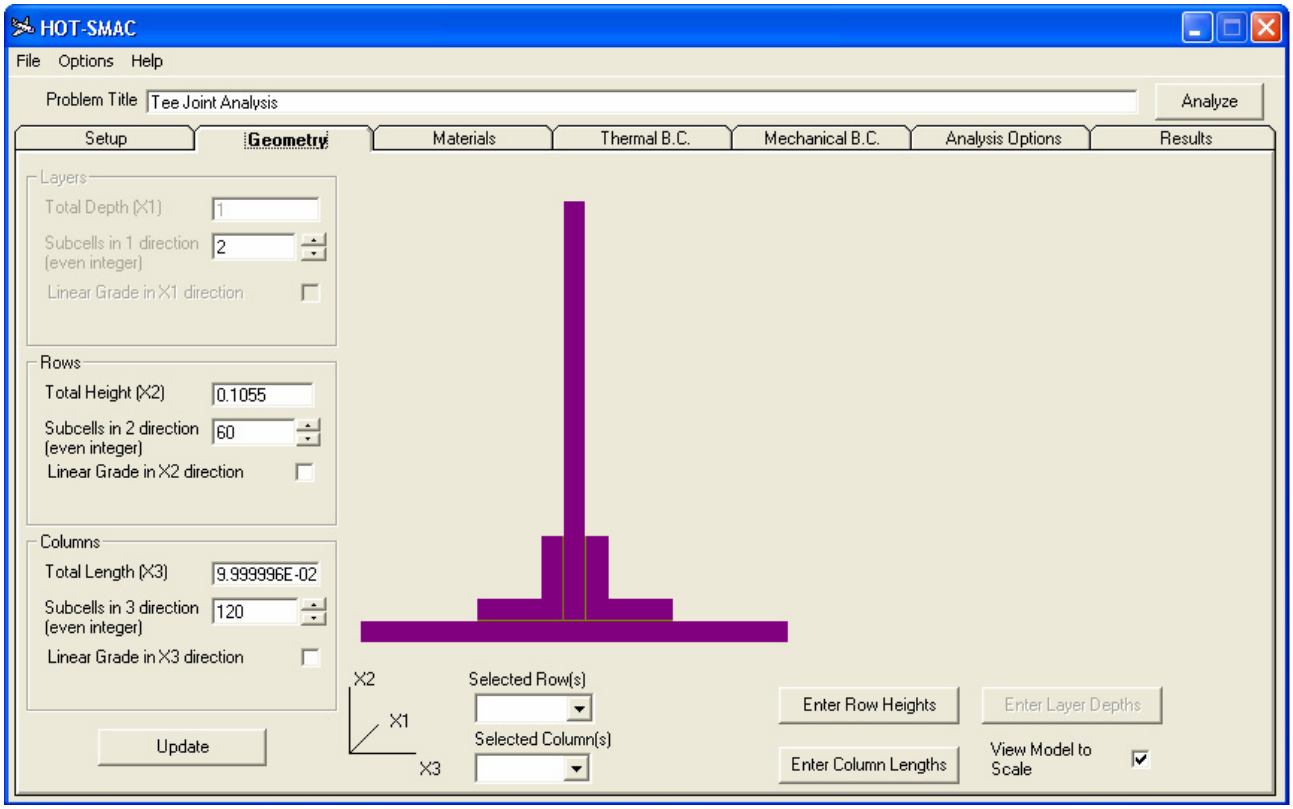

Fig. 3. Screen shot of the HOT-SMAC software.

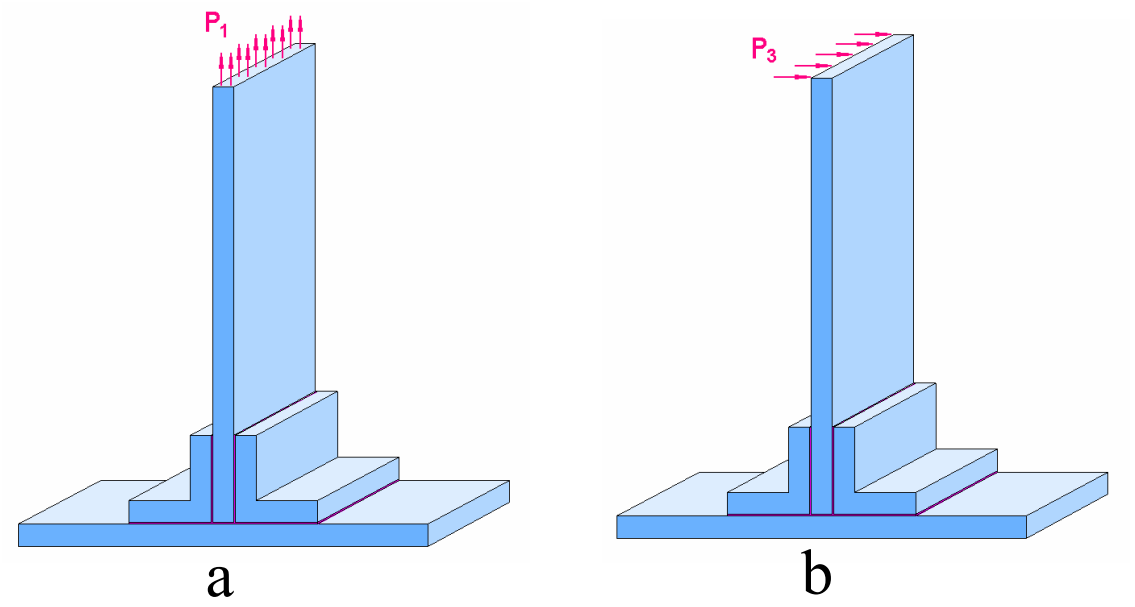

Fig. 4. Applied loading on the tee joint: a) Top face tensile loading (P_1); b) Side loading (P_3).

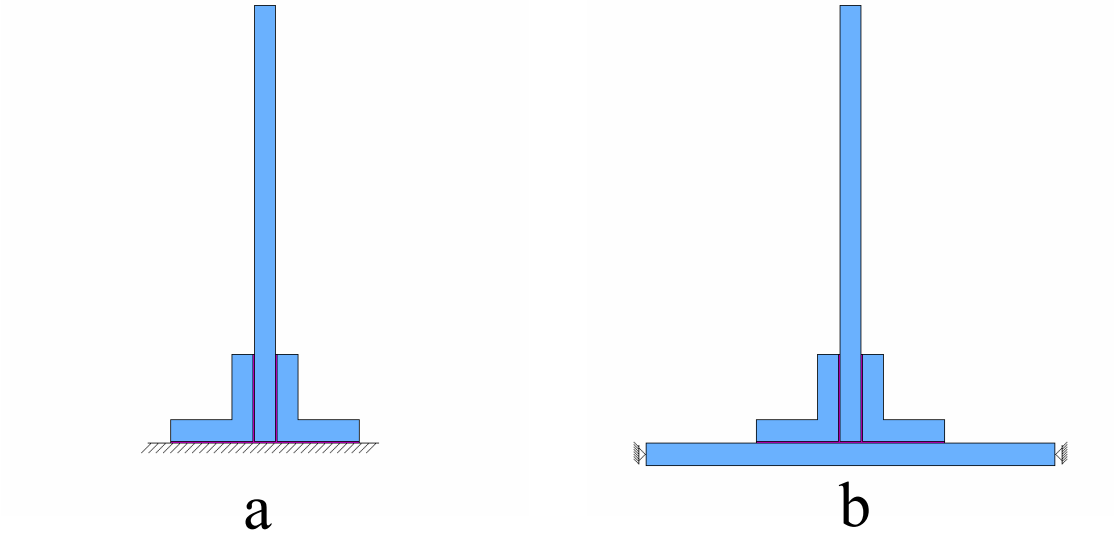

Fig. 5. Tee joint boundary conditions: a) Fixed Base; b) Flexible Base.

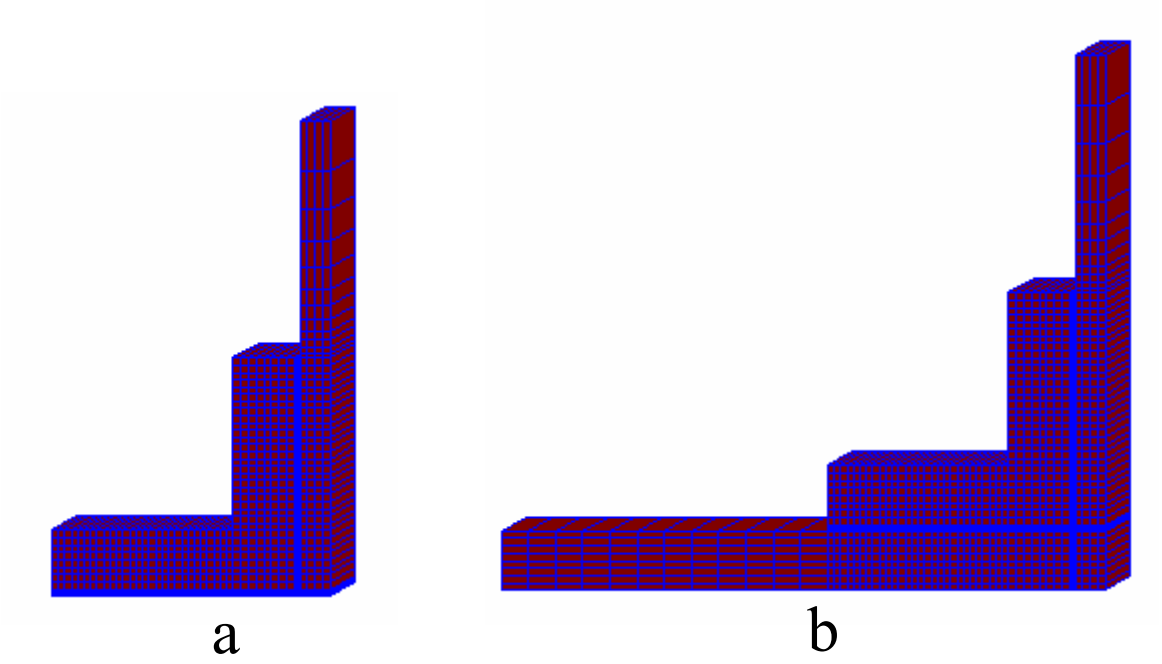

Fig. 6. HOT-SMAC subcell grid employed for top face tensile loading (P_1) for: a) Fixed base boundary conditions; b) Flexible base boundary conditions.

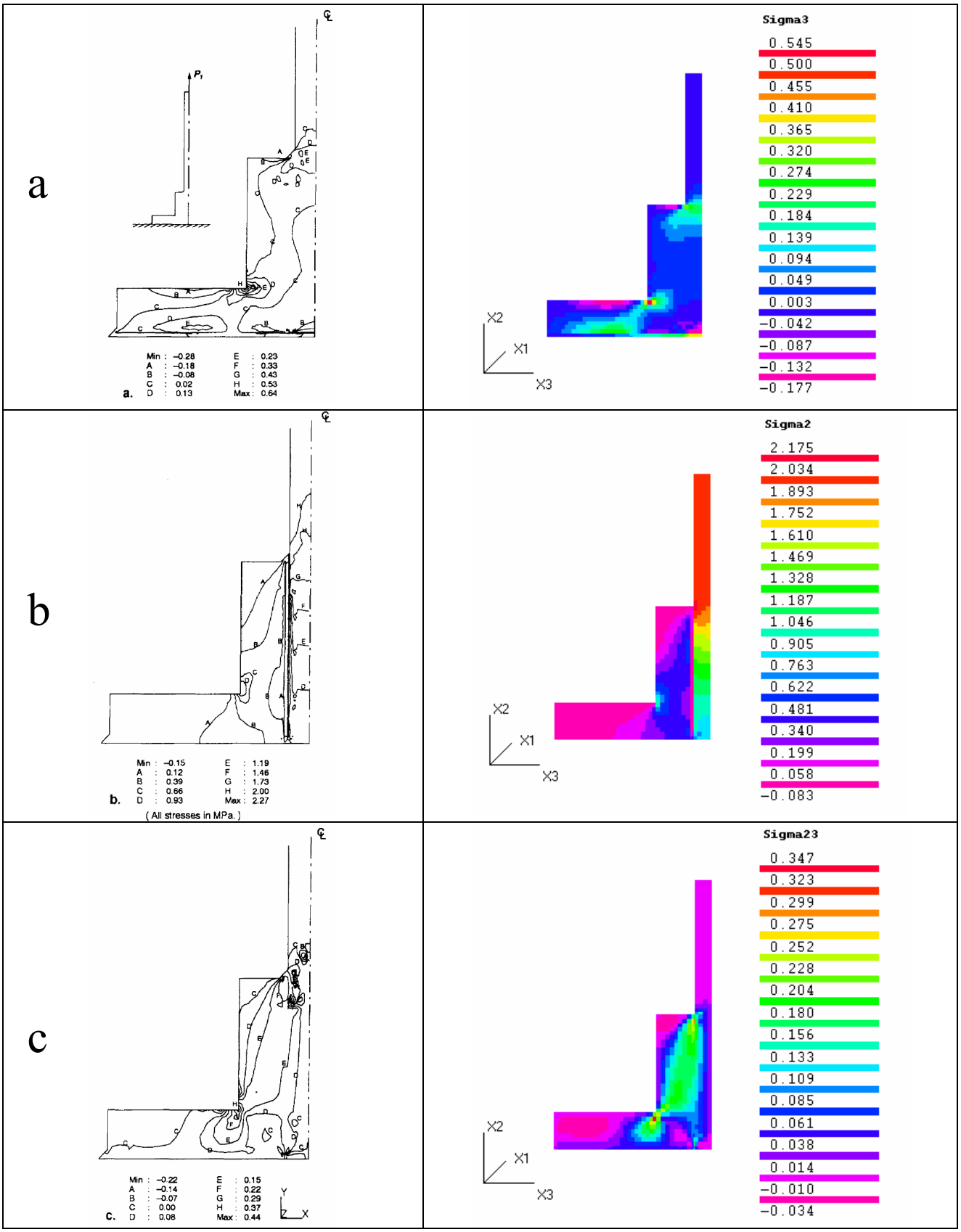

Fig. 7. Comparison of the HOT-SMAC stress component results with the FEA results of Apalak et al. (1996) for top face loading (P_1 = 5 N/mm) and fixed support. a) σ_{33}; b) σ_{22}; and c) σ_{23}.

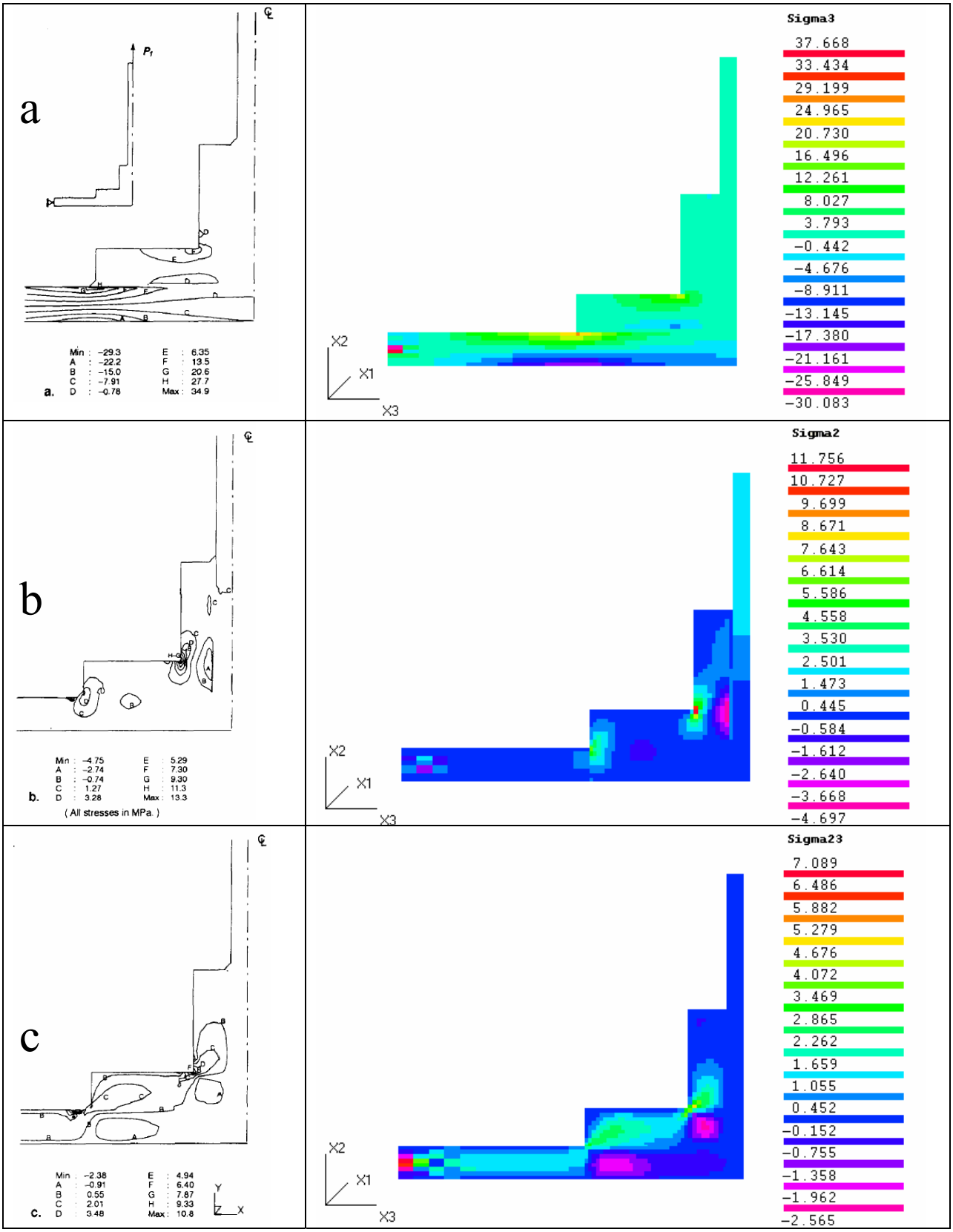

Fig. 8. Comparison of the HOT-SMAC stress component results with the FEA results of Apalak et al. (1996) for top face loading (P_1 = 5 N/mm) and flexible support. a) σ_{33}; b) σ_{22}; and c) σ_{23}.

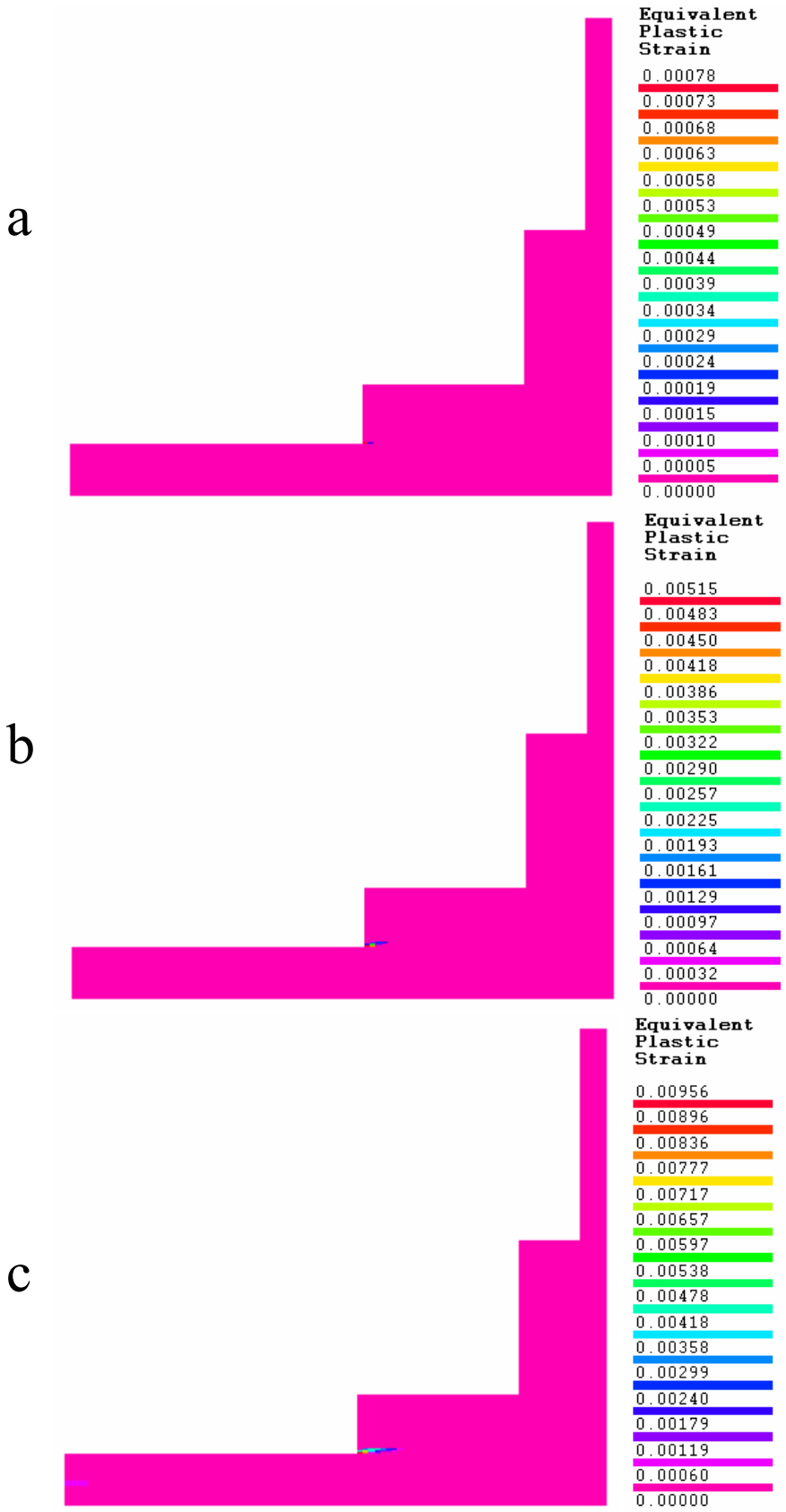

Fig. 9. Equivalent plastic strain fields in the top face loaded (P_1) tee joint with flexible base at applied load levels of: a) 30 N/mm; b) 40 N/mm; and c) 50 N/mm.

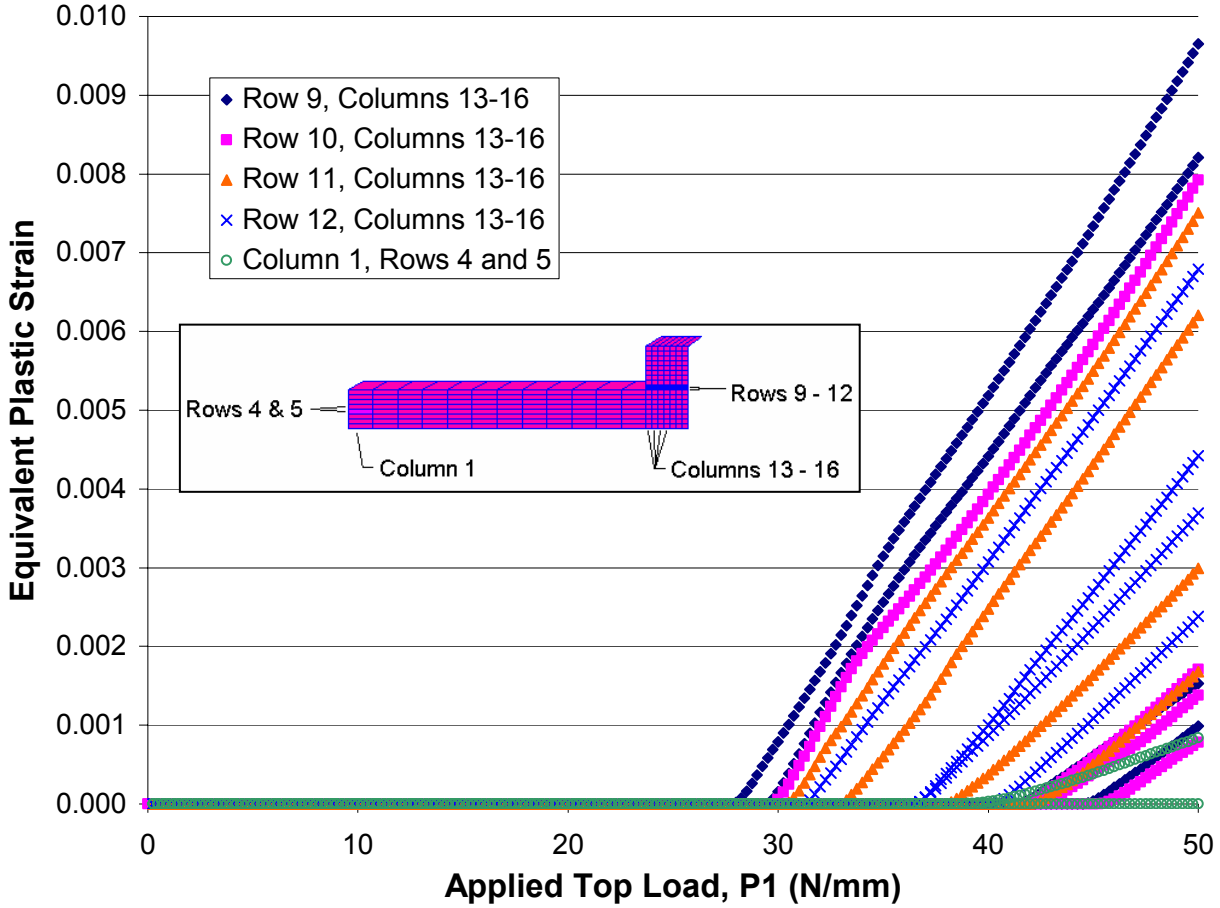

Fig. 10. Equivalent plastic strain evolution in adhesive subcells near the left face of the joint between the support and the horizontal plate (rows 9 – 12, columns 13 – 16) and in steel subcells to which the pinned boundary condition are applied (rows 4 & 5, column 1).

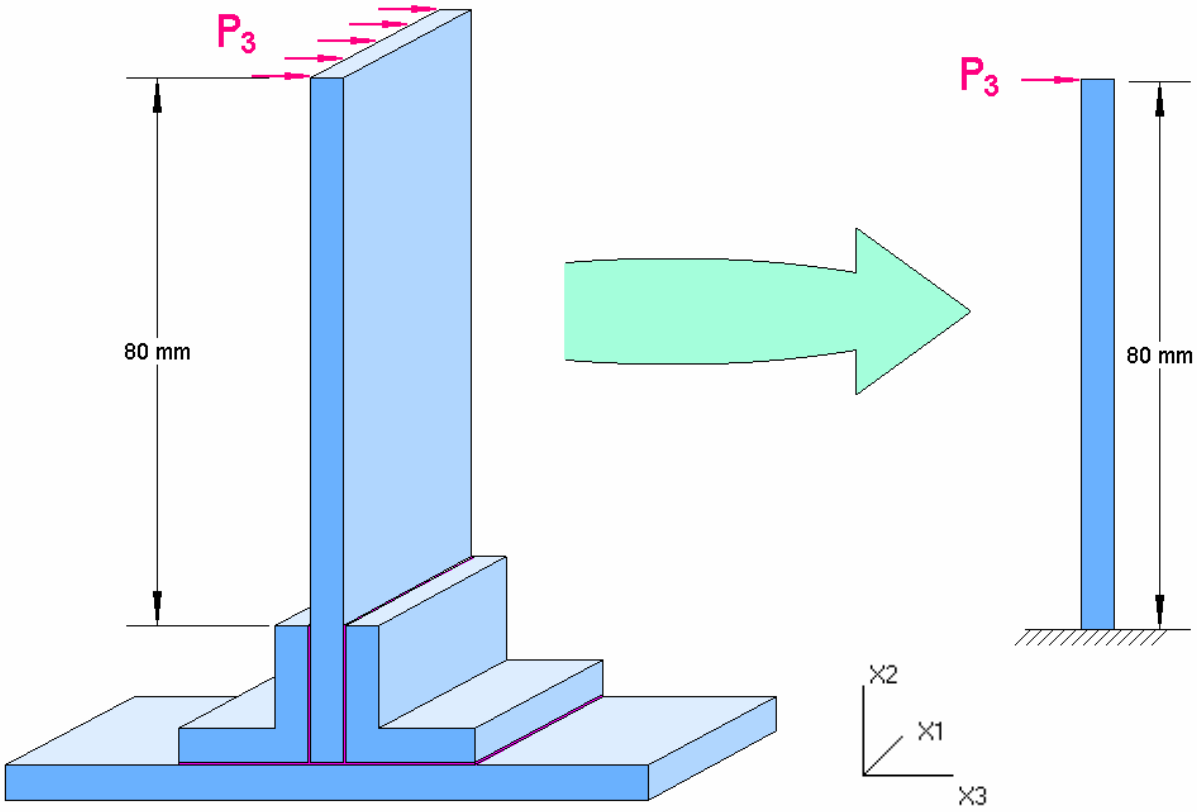

Fig. 11. The cantilever beam problem on the right serves as an upper bound on the elastic longitudinal stress in the vertical plate of the tee joint problem subjected to side loading.

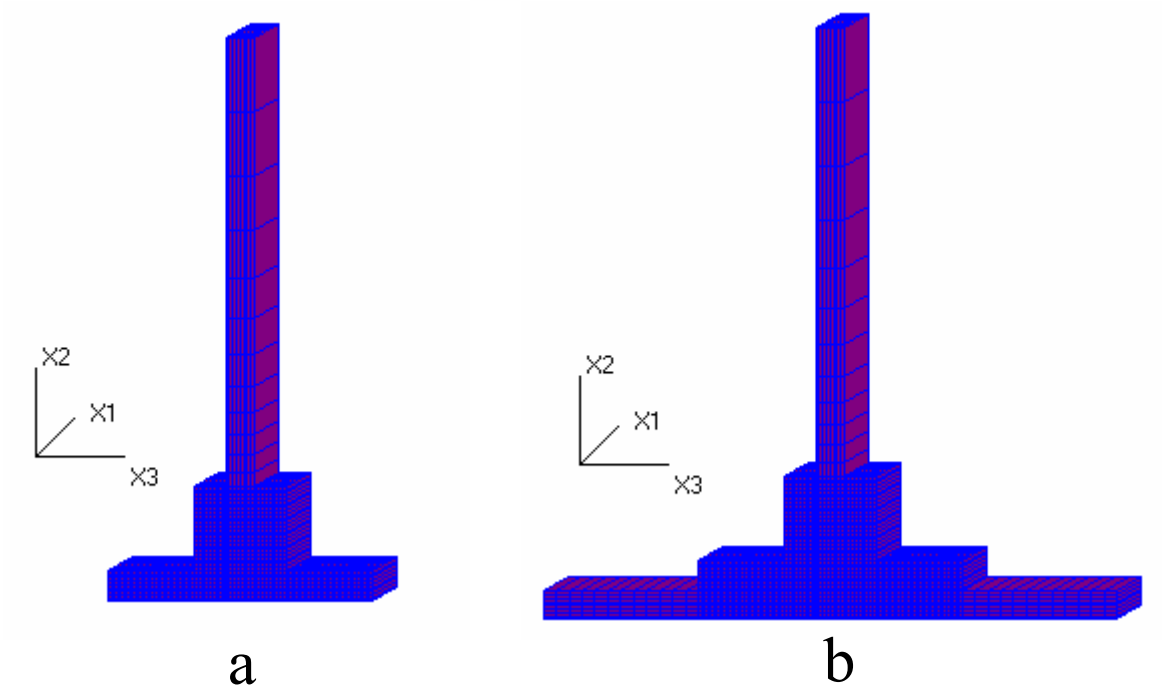

Fig. 12. HOT-SMAC subcell grids employed to model the response of the tee joint to side loading (P_3) in the case of: a) fixed support; b) flexible support.

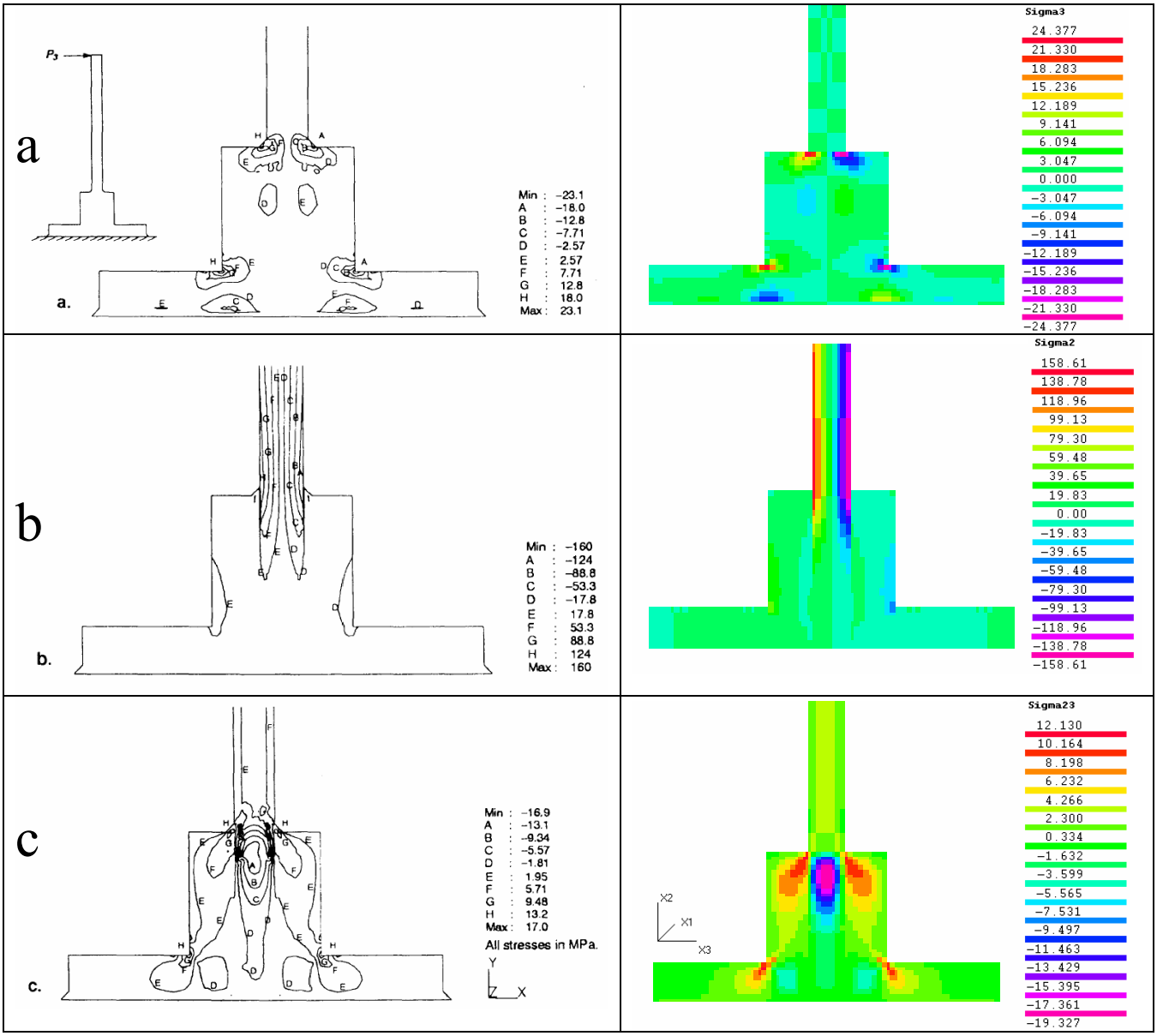

Fig. 13. Comparison of the HOT-SMAC stress component results with the FEA results of Apalak et al. (1996) for side loading (P_3 = 10 N/mm) and fixed base. a) σ_{33}; b) σ_{22}; and c) σ_{23}.

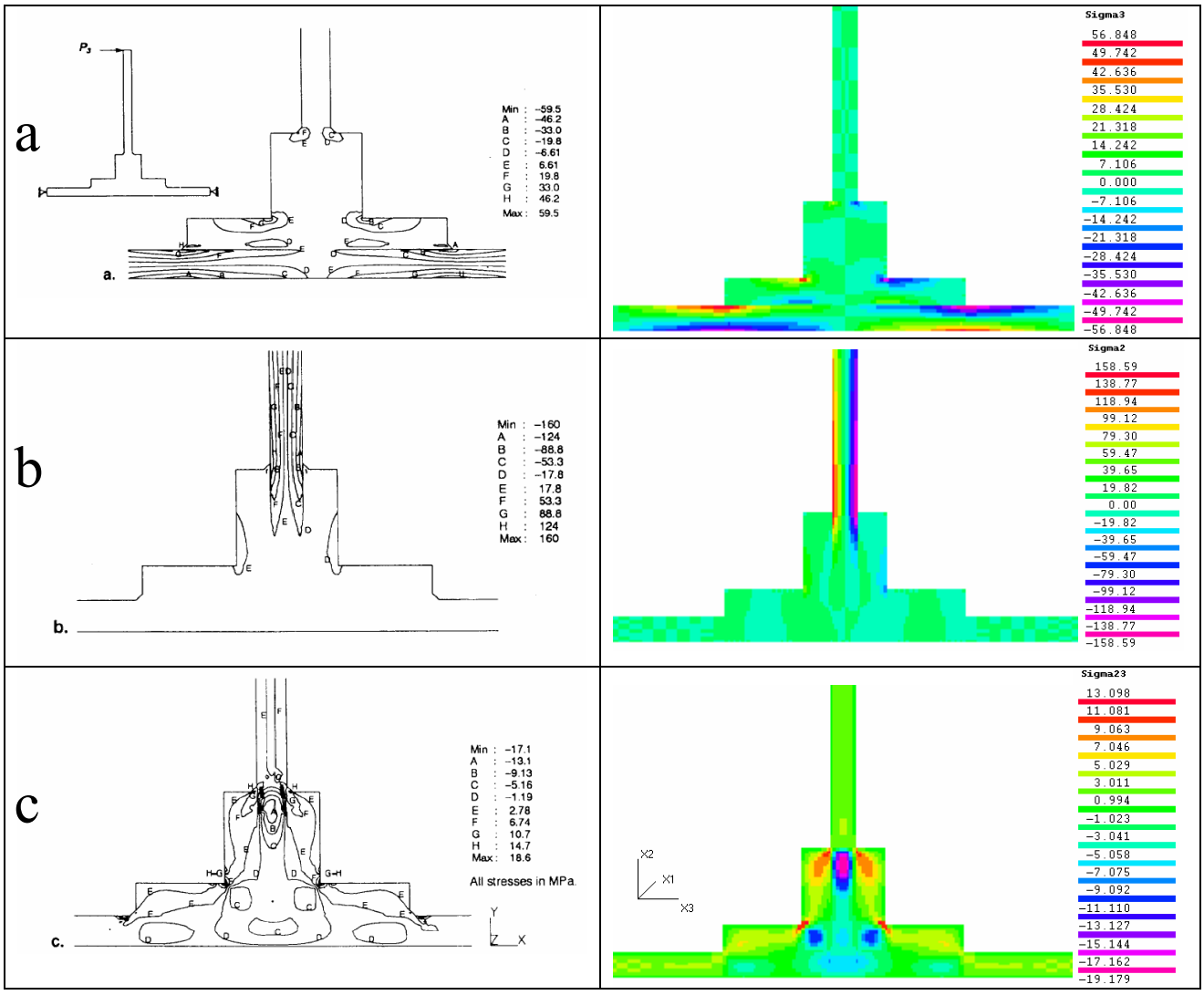

Fig. 14. Comparison of the HOT-SMAC stress component results with the FEA results of Apalak et al. (1996) for side loading (P_3 = 10 N/mm) and flexible base. a) σ_{33}; b) σ_{22}; and c) σ_{23}.

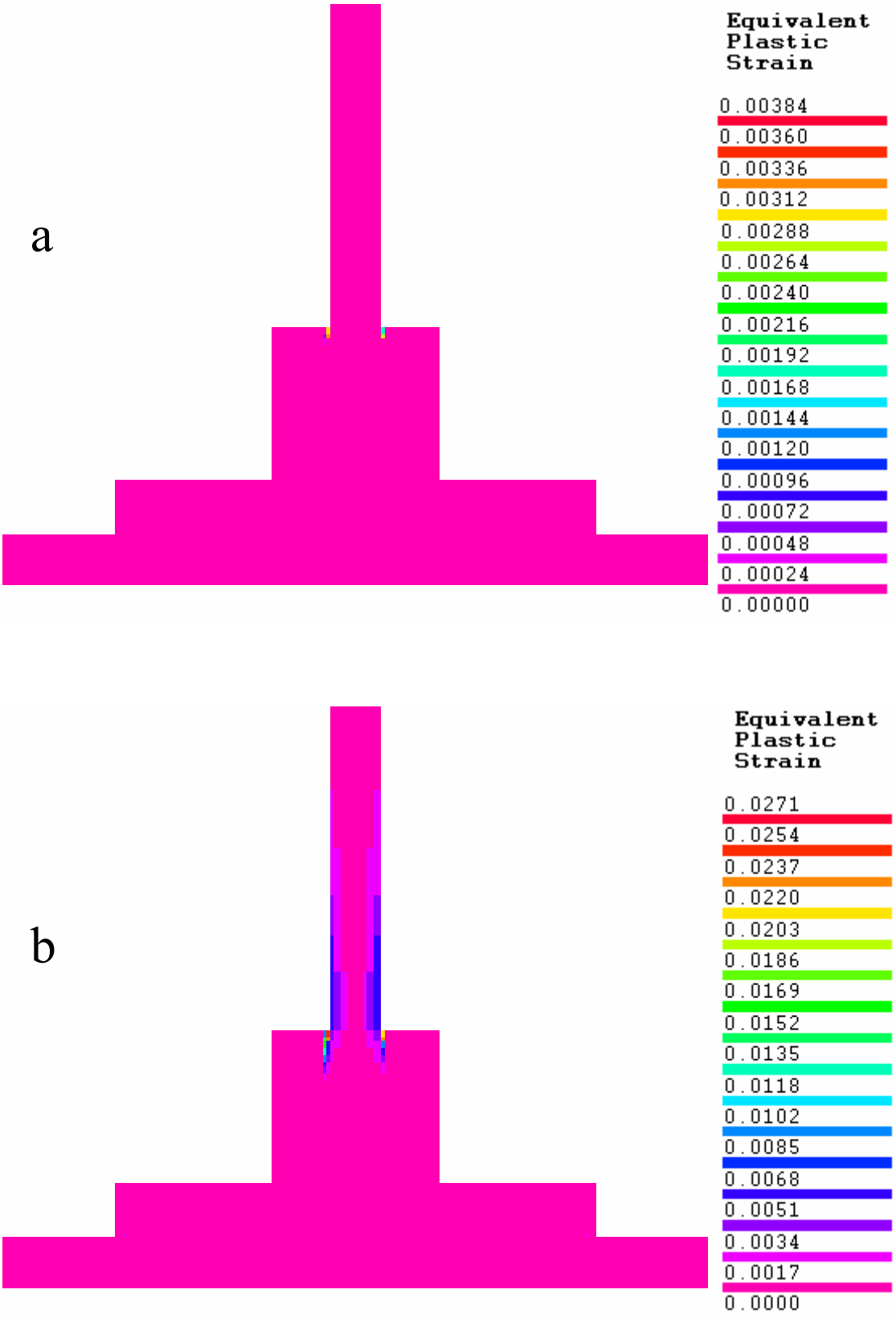

Fig. 15. Equivalent plastic strain fields in the side loaded (P_3) tee joint with flexible base at applied load levels of: a) 20 N/mm; b) 40 N/mm.

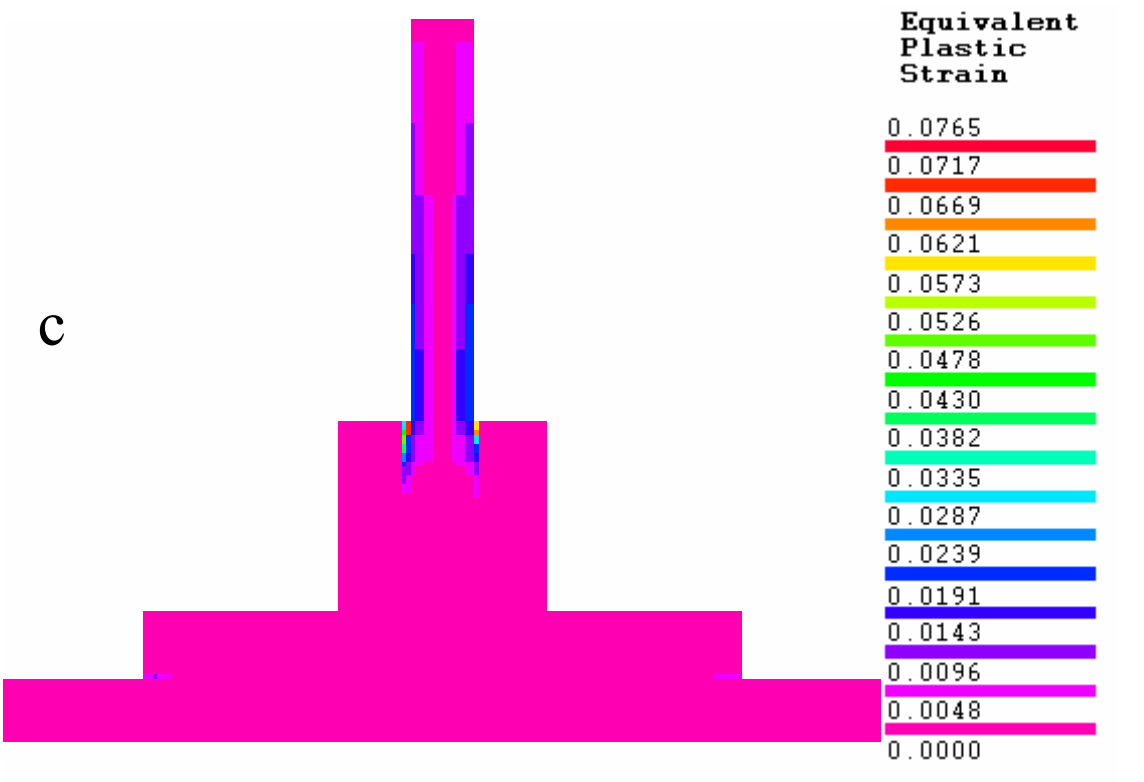

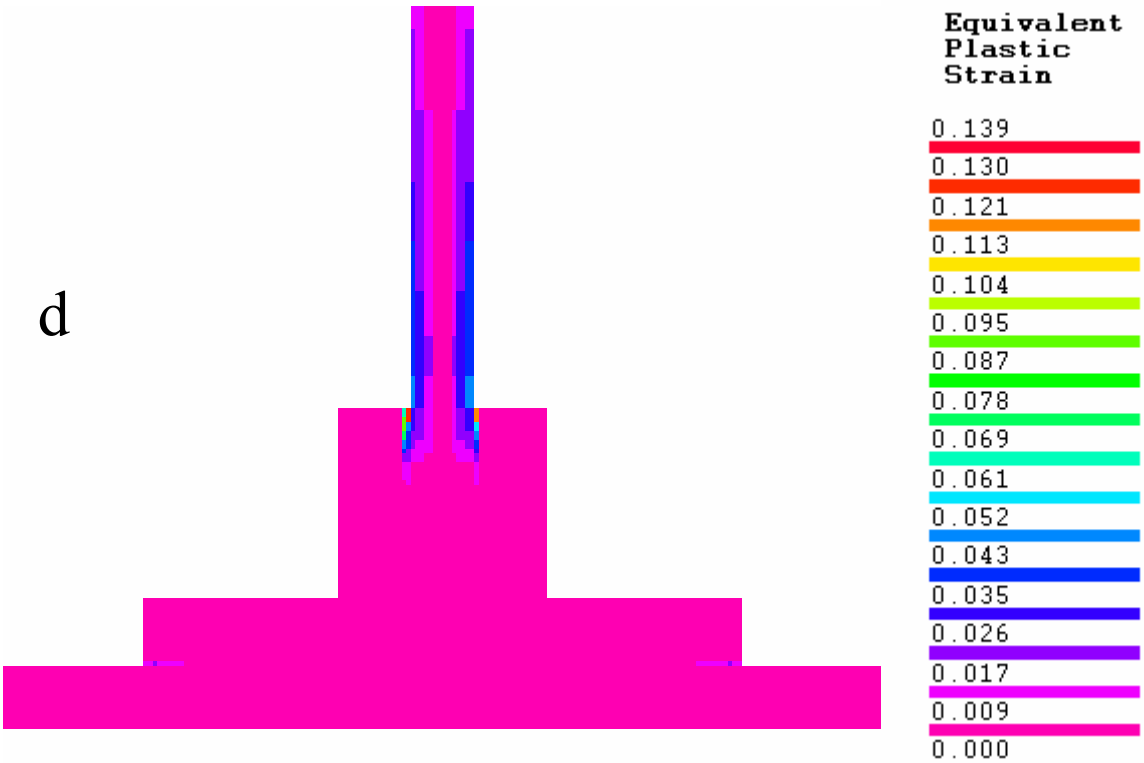

Fig. 15 (cont.) Equivalent plastic strain fields in the side loaded (P_3) tee joint with flexible base at applied load levels of: c) 40 N/mm; d) 60 N/mm.

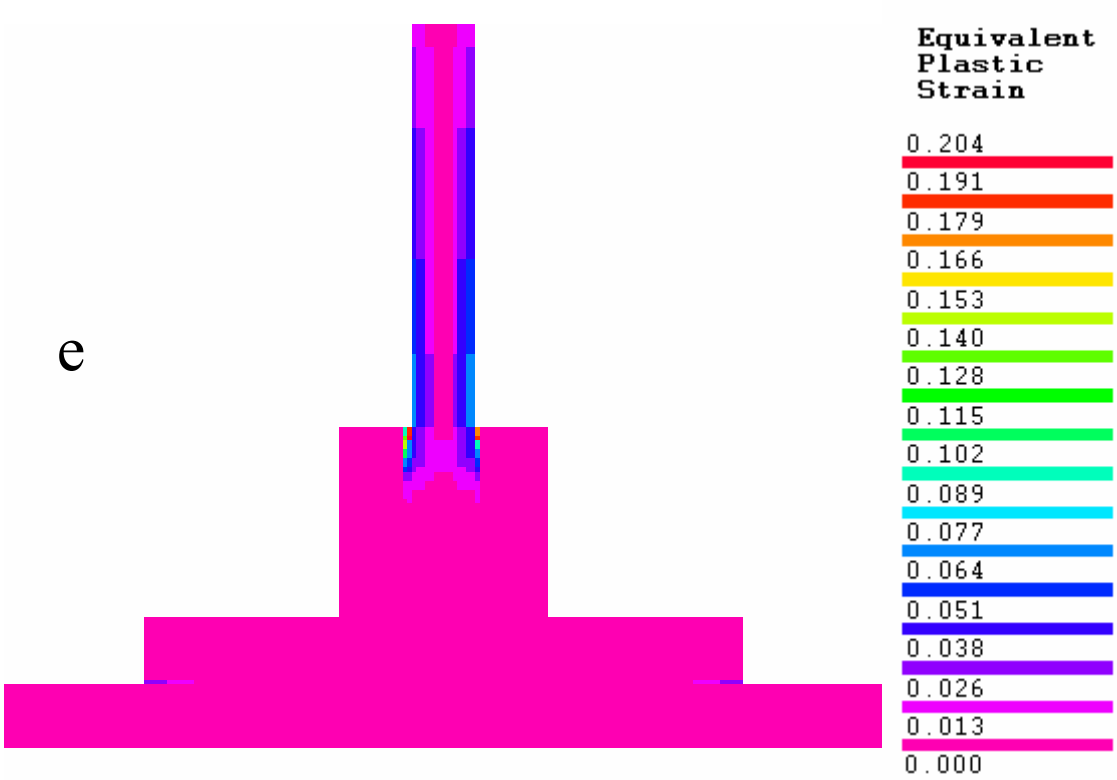

Fig. 15 (cont.) Equivalent plastic strain fields in the side loaded (P_3) tee joint with flexible base at applied load levels of: e) 100 N/mm.

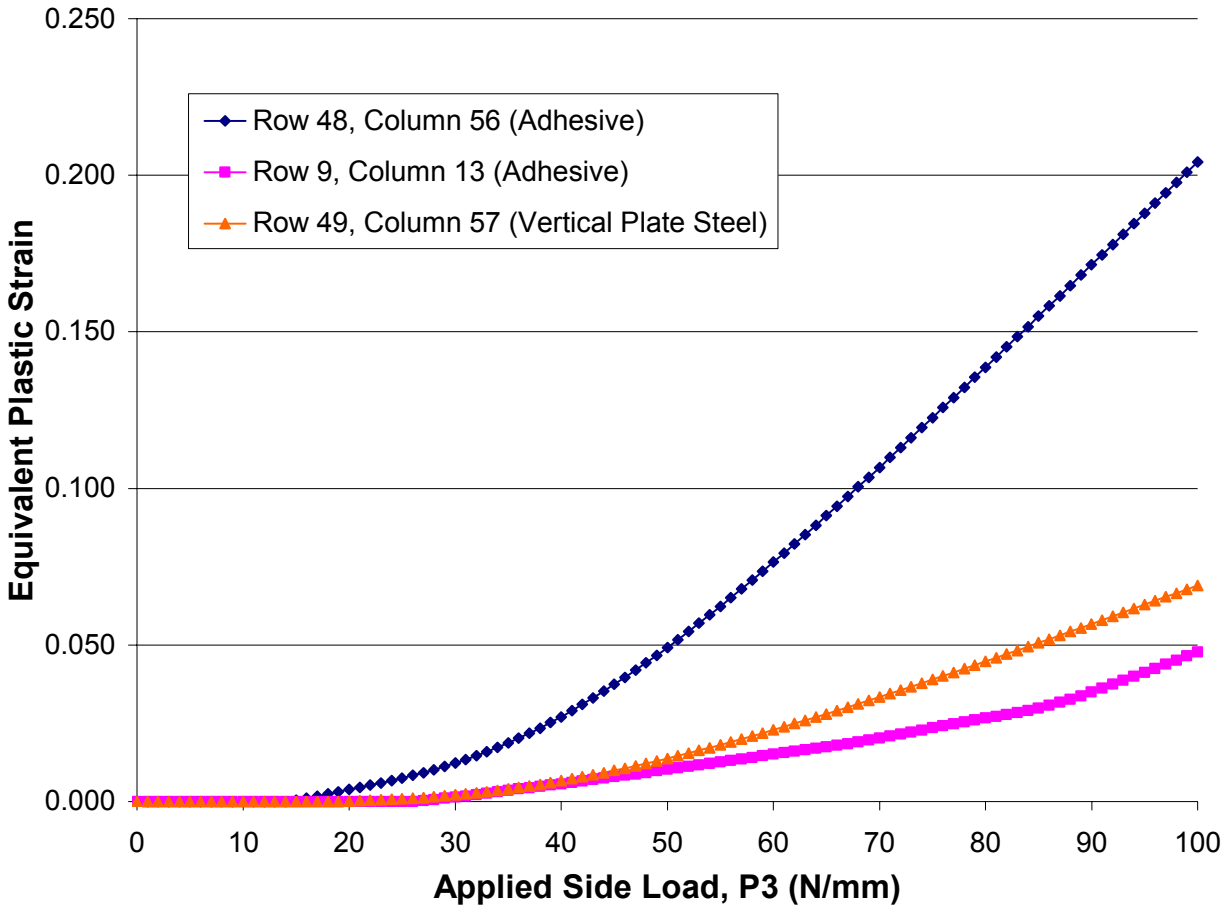

Fig. 16. Equivalent plastic strain evolution in an adhesive subcell at the top face of the joint between the support and the vertical plate (48, column 9), in an adhesive subcell at the left face of the joint between the support and the horizontal plate (row 9, column 13), and in a steel subcell in the vertical plate close to the top face of the support (rows 49, column 57).

REPORT DOCUMENTATION PAGE

Form Approved
OMB No. 0704-0188

1. AGENCY USE ONLY (*Leave blank*)	2. REPORT DATE	3. REPORT TYPE AND DATES COVERED
	May 2004	Final Contractor Report

4. TITLE AND SUBTITLE

Elasto-Plastic Analysis of Tee Joints using HOT-SMAC

5. FUNDING NUMBERS

WBS–22–708–87–07
NCC3–650

6. AUTHOR(S)

Brett A. Bednarcyk and Phillip W. Yarrington

7. PERFORMING ORGANIZATION NAME(S) AND ADDRESS(ES)

Ohio Aerospace Institute
22800 Cedar Point Road
Brook Park, Ohio 44142

8. PERFORMING ORGANIZATION REPORT NUMBER

E–14543

9. SPONSORING/MONITORING AGENCY NAME(S) AND ADDRESS(ES)

National Aeronautics and Space Administration
Washington, DC 20546–0001

10. SPONSORING/MONITORING AGENCY REPORT NUMBER

NASA CR–2004-213067

11. SUPPLEMENTARY NOTES

Brett A. Bednarcyk, Ohio Aerospace Institute, 22800 Cedar Point Road, Brook Park, Ohio 44142; and Phillip W. Yarrington, Collier Research Corporation, Harbour Centre, 2 Eaton Street, Suite 504, Hampton, Virginia 23669. Project Manager, Steve M. Arnold, Structures and Acoustics Division, NASA Glenn Research Center, organization code 5920, 216–433–3334.

12a. DISTRIBUTION/AVAILABILITY STATEMENT

Unclassified - Unlimited
Subject Category: 39 Distribution: Nonstandard

Available electronically at http://gltrs.grc.nasa.gov

This publication is available from the NASA Center for AeroSpace Information, 301–621–0390.

12b. DISTRIBUTION CODE

13. ABSTRACT ***(Maximum 200 words)***

The Higher Order Theory-Structural/Micro Analysis Code (HOT-SMAC) software package is applied to analyze the linearly elastic and elasto-plastic response of adhesively bonded tee joints. Joints of this type are finding an increasing number of applications with the increased use of composite materials within advanced aerospace vehicles, and improved tools for the design and analysis of these joints are needed. The linearly elastic results of the code are validated versus finite element analysis results from the literature under different loading and boundary conditions, and new results are generated to investigate the inelastic behavior of the tee joint. The comparison with the finite element results indicates that HOT-SMAC is an efficient and accurate alternative to the finite element method and has a great deal of potential as an analysis tool for a wide range of bonded joints.

14. SUBJECT TERMS

Bonded joints; Elastic; Plastic; Stress analysis; Adhesive joints, Micromechanics

15. NUMBER OF PAGES

31

16. PRICE CODE

17. SECURITY CLASSIFICATION OF REPORT	18. SECURITY CLASSIFICATION OF THIS PAGE	19. SECURITY CLASSIFICATION OF ABSTRACT	20. LIMITATION OF ABSTRACT
Unclassified	Unclassified	Unclassified	